Preprints of the 19th World Congress
The International Federation of Automatic Control
Cape Town, South Africa. August 24-29, 2014

Data-Driven Design of Sliding Mode Controllers for Ferroelectric Actuators

Jerry A. McMahan Jr. * **Ralph C. Smith** **

* *Department of Mathematics, North Carolina State University, Raleigh, NC 27695 USA (email: jamcmaha@ncsu.edu)*
** *Department of Mathematics, North Carolina State University, Raleigh, NC 27695 USA (email: rsmith@ncsu.edu)*

Abstract: Sliding mode controllers are frequently employed to track reference signals in the presence of model errors provided a worst-case bound on such errors is known. The uncertainty bound is often chosen through intuition or heuristic observations which can degrade control authority if the bound is too conservative. We describe a method for applying quantified parameter uncertainties obtained via Bayesian techniques to the design of sliding mode controllers. We illustrate the performance of this approach through numerical simulation in the context of ferroelectric actuator systems.

1. INTRODUCTION

Smith [2005] and Smith and Hu [2012] describe a wide range of applications for which ferroelectric materials have been considered, including nanopositioning stages, ultrasonic transducers, fuel injection valves, and engine components for nano-air vehicles. The reasons for using ferroelectric materials include properties such as low cost, broadband transduction capabilities, and dual sensor/actuator capabilities. Unfortunately, the nonlinear and hysteretic behavior inherent to these materials makes computationally efficient modeling difficult. One way around this difficulty is to employ a robust control method such as sliding mode control, which guarantees good performance assuming bounds on the modeling errors are known.

Examples of sliding mode controllers employed in smart material systems are found in Xu and Li [2009], Chen and Hisayama [2008], Liaw et al. [2007] and Sofla et al. [2010]. Although the bound on the system modeling error is a crucial component of the sliding mode control design, the literature often fails to describe precisely how this bound is chosen. A common approach to this problem is to use an adaptive method to select an appropriate error bound Monsees and Scherpen [2000], Yu et al. [2003], Plestan et al. [2010], which reduces the need for prior knowledge of the system uncertainty and can have advantages in reducing control activity. However, these methods typically require the system to satisfy additional assumptions to ensure convergence of the adaptive error, which may be difficult to verify.

The approach we employ in this paper was introduced in Crews et al. [2012] to control a shape memory alloy bending actuator. This method uses Bayesian inference to characterize the modeling uncertainty as a stochastic parameter in the model using measured data. The uncertainty bound is chosen according to a confidence interval associated with the probability distribution of the estimated random inputs to the model, so that the selected confidence quantifies the accuracy of the bound. Rather than requiring the designer to derive an accurate bound on the model error, this approach only requires an initial estimate of the measurement noise, which is typically easy to provide. Results in Crews et al. [2013] have verified the performance of this approach experimentally for the shape memory alloy actuator. Here, we apply this approach to a ferroelectric actuator model and compute simulation results to test for the desired behavior.

The remainder of the paper is organized as follows. First we summarize the ferroelectric actuator model, originally derived in Smith and Hu [2012]. We also summarize the inversion algorithm from McMahan et al. [2013] used to linearize the actuator model. Next we discuss the Bayesian framework for characterizing the uncertainty in the system and demonstrate this approach applied to the linearized ferroelectric actuator model using numerical simulation. In the following section, we define the sliding mode controller used for reference tracking, with the control parameters derived from the estimated distributions for the uncertain parameters. The expected closed-loop behavior for a sinusoidal reference signal is verified through numerical simulation.

2. MODEL DEVELOPMENT

2.1 Actuator Model

We consider the model

$$\begin{aligned}\dot{\varepsilon}(t) &= -\frac{A + s^E Lk}{s^E Lc}\varepsilon(t) + \frac{A}{s^E Lc}\varepsilon_{mat}[E, \sigma_0](t) \\ &= a\varepsilon(t) + b\varepsilon_{mat}[E](t), \end{aligned} \tag{1}$$

developed in Smith and Hu [2012] for a prestressed PZT actuator. Here A is the area of a cross-section of the actuator, L is the length of the actuator, s^E is a physical parameter of the actuator material, k is the actuator stiffness, c is the actuator damping coefficient, and $\varepsilon_{mat}[E, \sigma_0](t)$ the strain in the actuator material at time t in response to

[1] This research was supported in part by the Air Force Office of Scientific Research through the grant AFOSR FA9550-11-1-0152.

electric field input function E and the constant prestress σ_0. We have used operator notation to indicate that ε_{mat} is an operator mapping the time-dependent input functions E, σ_0 to the time-dependent output strain $\varepsilon_{mat}[E, \sigma_0]$ with $\varepsilon_{mat}[E, \sigma_0](t)$ denoting the output at time t. The prestress is constant, so we can consider it a parameter and treat the material strain as an operator on E only, simplifying the notation to $\varepsilon_{mat}[E](t)$.

Although a particular actuator model is described for concreteness, the general form of a linear model nonlinearly coupled to an input can be successfully applied to a variety of actuator models.

2.2 Homogenized Energy Model

The strain in the material $\varepsilon_{mat}[E](t)$ is specified by the homogenized energy model for hysteretic ferroelectric materials developed in Smith and Hu [2012] which we summarize here. We represent the material strain as

$$\varepsilon_{mat}[E](t) = s^E \sigma_0 + d[E](t)E(t) + \varepsilon_{irr}[E](t), \quad (2)$$

with the E-dependent piezoelectric strain coefficient $d[E](t)$ and the irreversible strain $\varepsilon_{irr}[E](t)$ written as

$$\begin{aligned} d[E](t) &= \int_0^\infty \int_{-\infty}^\infty \overline{d}[E](t, E_I, F_c)\nu_I(E_I)\nu_c(F_c)\, dE_I\, dF_c \\ \varepsilon_{irr}[E](t) &= \int_0^\infty \int_{-\infty}^\infty \overline{\varepsilon}_{irr}[E](t, E_I, F_c)\nu_I(E_I)\nu_c(F_c)\, dE_I\, dF_c. \end{aligned} \quad (3)$$

These integrals describe the macroscopic outputs $d[E](t)$ and $\varepsilon_{irr}[E](t)$ as weighted averages of local outputs $\overline{d}[E](t, E_I, F_c)$ and $\overline{\varepsilon}_{irr}[E](t, E_I, F_c)$. These integrals are computed with respect to the variables E_I, F_c over their respective domains $(-\infty, \infty)$ and $(0, \infty)$. The interaction electric field E_I quantifies local electrical effects that augment the input field E and the critical thermodynamic driving force F_c specifies the energy required for transitions between dipole orientations to occur (and thus determines the local hysteresis width). The densities $\nu_I(E_I), \nu_c(F_c)$ weight the local outputs corresponding to each value of E_I, F_c. These densities are identified with the particular material being used and effectively specify the finite subset of the domain of E_I, F_c for which local effects are significant, ensuring the improper integrals converge. For computational purposes, the densities are approximated by a weighted sum of normal and lognormal densities.

The local outputs $\overline{d}[E](t, E_I, F_c), \overline{\varepsilon}_{irr}[E](t, E_I, F_c)$ are expressed as

$$\begin{aligned} \overline{d}[E]\,(t, E_I, F_c) &= \sum_{\alpha=+,-,90} d_\alpha x_\alpha[E]\,(t, E_I, F_c) \\ \overline{\varepsilon}_{irr}[E]\,(t, E_I, F_c) &= \sum_{\alpha=+,-,90} \varepsilon_R^\alpha x_\alpha[E]\,(t, E_I, F_c) \end{aligned} \quad (4)$$

where $x_\alpha[E](t, E_I, F_c)$ is the fraction of dipoles in orientation α (where α is positive, negative, or 90°) at time t corresponding to the parameters E_I, F_c and input function E, d_α is the piezoelectric constant for each dipole orientation, and ε_R^α is the remanence polarization for each dipole orientation. The local outputs are thus given by a sum of the output values for each dipole orientation weighted by the fraction of dipoles in those orientations.

The dipole fractions are described by the evolution equation

$$\begin{aligned} \dot{x}_+ &= -p_{+90}\big(E_e(t), F_c\big)x_+ + p_{90+}\big(E_e(t)\big)x_{90} \\ \dot{x}_{90} &= p_{+90}\big(E_e(t), F_c\big)x_+ p_{-90}\big(E_e(t), F_c\big)x_- \\ &\quad -\big[p_{90+}\big(E_e(t), F_c\big) + p_{90-}\big(E_e(t), F_c\big)\big]x_{90} \\ \dot{x}_- &= p_{90-}\big(E_e(t), F_c\big)x_{90} - p_{-90}\big(E_e(t), F_c\big)x_- \end{aligned} \quad (5)$$

where $E_e(t) = E(t) + E_I$ is the effective input electric field, $p_{\alpha\beta}$ is the transition rate from dipole orientation α to dipole orientation β and the dot denotes differentiation with respect to time. We have suppressed the notation of dependencies of x_α to simplify the notation. The equation given assumes only 90° switching occurs between dipole orientations (i.e., there is no switching directly from positive to negative orientations or vice-versa). Note the equation can be reduced using the fact that $x_+ + x_{90} + x_- = 1$. For more detailed information on the dipole fraction equations, the reader is referred to Smith and Hu [2012].

Although the details are omitted here, the homogenized energy model is physically derived via the principle of energy minimization. Not only does this provide a physical interpretation for the model and its parameters, but it highlights the mathematical analogies between models for materials which behave similarly but rely on different physical mechanisms (e.g., shape memory alloys) by minimizing different types of energy functionals.

2.3 Homogenized Energy Model Inversion Algorithm

The model (1) is a linear system coupled nonlinearly to the input field, E. Suppose we are given an approximate right inverse ε_{mat}^{-1} for ε_{mat} so that letting $E = \varepsilon_{mat}^{-1}u$ we obtain $\varepsilon_{mat}\varepsilon_{mat}^{-1}u = u + e \approx u$. This inverse operator allows the actuator system to be approximately linearized to obtain the equation

$$\begin{aligned} \dot{\varepsilon}(t) &= a\varepsilon(t) + b\varepsilon_{mat}[\varepsilon_{mat}^{-1}[u]](t) \\ &= a\varepsilon(t) + bu(t) + be[u](t) \\ &\approx a\varepsilon(t) + bu(t), \end{aligned} \quad (6)$$

where $e[u](t) = b\varepsilon_{mat}[\varepsilon_{mat}^{-1}[u]](t) - bu(t)$ is the inversion error. As long as the inversion error be can be compensated, u is approximately equal to the strain due to the material (i.e., $u \approx \varepsilon_{mat}[E]$). The ability to directly specify the material strain as an input allows for simpler control design.

We use a simple, efficient algorithm from McMahan et al. [2013] for inverting ε_{mat} which is based on a bisection method calculated sequentially in time. The following steps summarize the algorithm:

(1) Set the current time t_k and the time at which the model is to be computed t_{k+1}. Choose a bounded input range for the input field so that the function $E(t_k) \to \varepsilon_{mat}[E](t_{k+1})$ is monotone (e.g., the restrict the input to some bounded non-negative interval). Choose an error bound for e.
(2) Choose a number of points, N, and divide the input range into N equally spaced points.

(3) Input a desired value ε^d_{mat} for the material strain and initialize $E(t_k)$ to the midpoint of the input range.
(4) Compute the output $\varepsilon_{mat}[E](t_{k+1})$ and output error $\varepsilon^{err}_{mat} = \varepsilon_{mat}[E](t_{k+1}) - \varepsilon^d_{mat}$
(5) If $|\varepsilon^{err}_{mat}|$ is smaller than the error tolerance chosen in the first step, then save the current value of $E(t_k)$ as the result and save the state of the dipole fractions computed when calculating $\varepsilon_{mat}[E](t_{k+1})$.
(6) If $|\varepsilon^{err}_{mat}|$ is larger than the error tolerance, then remove the lower half of the input range if $\varepsilon^{err}_{mat} < 0$ or the upper half if $\varepsilon^{err}_{mat} > 0$. Set $E(t_k)$ to the midpoint of the resulting range and repeat the process from step 4 until the input points are exhausted or the tolerance is met.

For a given set of time nodes $t_0, \ldots, t_n$, initial values for the dipole fractions at t_0, and desired outputs $\varepsilon^k_{mat}, k = 1, \ldots, n$, applying this algorithm at each time interval results in input values $E^k = E(t_k), k = 0, \ldots, n-1$ so that an input signal interpolated over these values approximately satisfies $\varepsilon^k_{mat} = \varepsilon_{mat}[E](t_{k+1})$, $k = 0, \ldots, n-1$. The result is an approximate right inverse to ε_{mat}. The computational cost of this algorithm is less than or equal to $\mathcal{O}(\log_2(N-1))$ times the computational cost of computing $E(t_k) \to \varepsilon_{mat}[E](t_{k+1})$. Note that reasonable error tolerances can be achieved in practice for moderate values of N (e.g., $N = 129$ or $N = 257$ is used in many of the simulations in McMahan et al. [2013]).

3. PARAMETERIC UNCERTAINTY QUANTIFICATION

It is generally impossible in practice to completely eliminate modeling errors. As such, techniques which quantify the model error are useful as this additional information can be used to improve designs based on the model. In many cases, stochastic methods are a good fit for this problem, due to the approximately random nature of errors for well-modeled systems. The Bayesian framework for parameter estimation is one such method. Whereas deterministic model calibration computes a single set of values for the model parameters which result in a best fit of the model to the noisy measurements in some sense (e.g., least squares of data residuals), the Bayesian framework treats the model parameters as random variables and computes the associated probability densities to give best fit to the noisy measurements while taking into account prior beliefs about the values of the densities. Once these densities are computed, they can be used to compute the interval of model outputs at each time corresponding to some confidence probability. These intervals indicate the output range in which the data is expected to lie up to the chosen probability. For example, for a confidence interval of 95%, one would expect 95% of all measurements to lie within the confidence interval computed at the time the measurement was taken. We briefly outline the approach here and refer the reader to Smith [2014] and Stuart [2010] for more information on Bayesian inverse problems for uncertainty quantification.

For the model (6) we have

$$\frac{d\varepsilon}{dt}(t,\omega) = a(\omega)\varepsilon(t,\omega) + b(\omega)u(t), \tag{7}$$

where a and b are random variables and ω is the variable parameterizing the outcome space. Each parameter $a(\omega), b(\omega)$ has a probability density $p_a(\omega), p_b(\omega)$ which weights the range of parameter values.

The crucial relation in computing the optimal densities (i.e., the "best fit" in the Bayesian framework) is Bayes' rule

$$\pi(q|y) = \frac{p(y|q)\pi_{pr}(q)}{\int_{\mathbf{R}^d} p(y|q)\pi_{pr}\, dq} \tag{8}$$

which updates the current beliefs or assumptions about the parameter densities (i.e., the prior density $\pi_{pr}(q)$) using the current observations y to obtain the posterior density $\pi(q|y)$. Here $q = [q_1 \cdots q_d]^T$ is the vector of random parameters, $y = [y_1 \cdots y_N]^T$ is the observed experimental data collected at times $t_1, \ldots, t_N$, and

$$p(y|q) = \frac{1}{(\sigma\sqrt{2\pi})^N} \exp\left(-\frac{\|y - y(q)\|_2^2}{2\sigma^2}\right) \tag{9}$$

is the likelihood of observing y given q. In the expression for the likelihood, $y(q) = [y(t_1;q) \cdots y(t_N;q)]$ is the vector of the model output taken at times $t_1, \ldots, t_N$ with parameters q, $\|\|_2$ is the vector 2-norm in $\mathbf{R}^N$, and σ^2 is the measurement error variance. The measurement errors are assumed independent and identically distributed (iid) with mean 0. Also note that the form of the prior used in (9) implies that we are assuming the measurement error is normally distributed.

The value of σ can be estimated from observations of the error between measurement data and the model output from a deterministic model fit. For example, one might take the maximum absolute error between the deterministic model fit and measurement data, equate this to 2σ, and solve for σ to obtain a reasonable approximation, as 2σ corresponds to an approximately 95% confidence interval for Gaussian noise. If one is more certain the data will never exceed this maximum observed absolute error, then it may be more appropriate to use 3σ instead as this corresponds to approximately 99% confidence (or other multiples for various degrees of confidence in the data). This approach of specifying a fixed, reasonably accurate estimate for σ corresponds most closely to the scenario we are simulating. Note that it is also possible to formulate the Bayesian inverse problem to include σ as an uncertain model parameter (i.e., a random variable) and compute estimates of of its density (see Smith [2014] for details) without altering the way the computed model parameter densities are used in designing the control.

Let us emphasize a distinction between the roles of the random variables in this framework. The measurement error is represented as a random variable to model the inherent error and variability of the physical measurements. Although the model parameters are also random variables, this choice does not directly model any physical variability in the parameters. Rather, the model parameter densities assign values that represent the belief in the likelihood that any particular set of model parameters in the range of possible values fits the data in a way that is consistent with Baye's rule (8).

Figure 1 illustrates this with a hypothetical fit of lines to noisy data. There are multiple data points which may be

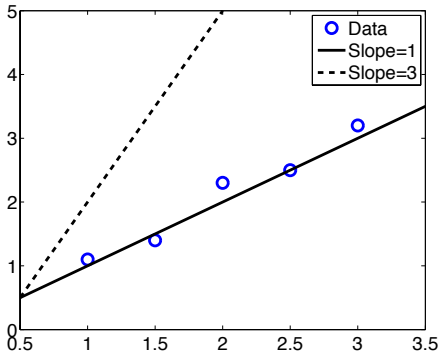

Fig. 1. Illustration of model parameter likelihoods. The probability density for the slope parameter would have a larger likelihood at the outcome associated with slope 1 than the outcome associated with slope 2 due to its closer agreement with the data.

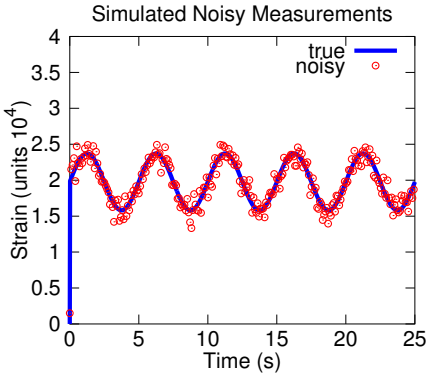

Fig. 2. Simulated noisy measurements used to calculate the density for the actuator model parameter a.

thought of as having random fluctuations that are characterized by the properties of the random variable chosen to model them (i.e., the variance). The model parameter for the line fit is the slope. Let $k(\omega)$ be the random variable for the slope, $p_k(\omega)$ the associated probability density, and let ω_1, ω_2 be the outcomes where $k(\omega_1) = 1, k(\omega_2) = 3$ (i.e., outcomes associated with the illustrated slopes). One would expect $p_k(\omega_1)$ to be relatively large due to the agreement between the data and the line with slope 1 and $p_k(\omega_2)$ to be small due to the poor fit of the line with slope 3. Note that the outcome parameters are simply a mathematical tool for mapping the slope value to the density value in a general way and do not in this case represent separate trials of an experiment or similar notions associated with the word "outcome".

We apply the Bayesian framework to the actuator model (7). For simplicity, assume b is known and take a to be a random parameter so that $q(\omega) = [a(\omega)]^T$ with $d = 1$. We compute the exact output of the model in response to a sinusoidal input and add synthetically generated Gaussian noise with zero mean and standard deviation $\sigma = 10^{-6}$ to the result to simulate measurement noise. The parameter values used are $a = -1.1372 \times 10^5$ and $b = 1.1237 \times 10^5$. Figure 2 shows the results.

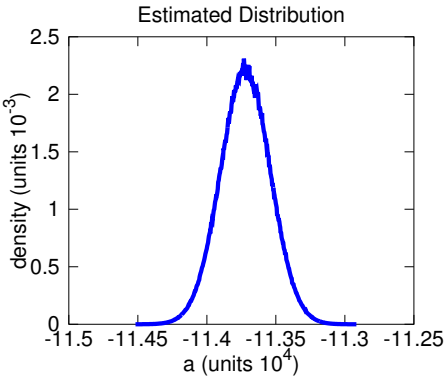

Fig. 3. Posterior distribution for the actuator model parameter a.

The sample problem has $d = 1$ random parameters which is small enough for the integral $\int_{\mathbf{R}^d} p(y|q)\pi_{pr}\, dq$ in the denominator of (8) to be evaluated practically with quadrature techniques. The resulting posterior distribution is shown in Figure 3. For models with large numbers of parameters (i.e., d large), approximation via numerical quadrature is impractical as the computational costs rise exponentially with the number of parameters. A popular approach to address this difficulty is to use a Markov Chain Monte Carlo (MCMC) method. These methods construct a Markov chain which has the posterior distribution as its equilibrium distribution, bypassing the need for directly evaluating the integral in the denominator. This approach is used in Crews et al. [2012] to estimate the parameters for a shape-memory alloy system and in Hu et al. [2013] to estimate the parameters for an actuator constructed from macro-fiber composites.

4. CONTROL DESIGN

4.1 Sliding Mode Control Design

Classical sliding mode control algorithms perform robustly provided bounds on the modeling errors are known (see Utkin [1992], Slotine and Li [1991]). The control law for these controllers contains a discontinuous component which increases with the size of the model error bounds. Large discontinuities in the input due to large model error bounds can excite unmodeled high frequency modes in the system, so it is important that these bounds be no larger than necessary for accuracy. The approach of using the parameter density obtained from the Bayesian estimation techniques described above was introduced in Crews et al. [2012] for the control of a shape-memory alloy bending actuator. Here we apply a similar strategy for the ferroelectric system described above.

Since we are considering a as the only parameter with non-negligible uncertainty, we rewrite the linearized actuator model (6) as

$$\dot{\varepsilon} = \overline{a}\varepsilon + bu + \Delta a\varepsilon$$

where $\overline{a}$ is the nominal value for a and Δa represents the deviation from $\overline{a}$. A natural way to incorporate the information obtained from Bayesian parameter estimation is to set $\overline{a}$ to the expectation of a (i.e., to $\int_{\mathbf{R}} a\pi(a|y)\, da$) and to calculate a bound on Δa based on a chosen confidence level. For the posterior distribution shown in

Figure 3, this yields $\overline{a} = -1.1372 \times 10^5$. To correspond to a 95% confidence level, the value of Δa_{max} is taken so that $\int_{\overline{a}-\Delta a_{max}}^{\overline{a}+\Delta a_{max}} \pi(a|y)\, da = 0.95$, which yields $\Delta a_{max} \approx 356$.

We design a standard sliding mode controller by defining the constraint function

$$s(e_1(t), e_2(t)) = \lambda e_1(t) + e_2(t)$$

where $\lambda > 0$ is a design parameter affecting the speed of convergence to the reference trajectory and $e_1(t) = \int_0^t (\varepsilon(z) - \varepsilon_r(z))\, dz$ and $e_2(t) = \varepsilon(t) - \varepsilon_r(t)$ are the cumulative error and error from the reference trajectory $\varepsilon_r(t)$. A Lyapunov-like function is defined so that

$$\begin{aligned}\frac{d}{dt}\frac{s(e_1,e_2)^2}{2} &= s(e_1,e_2)\dot{s}(e_1,e_2) \\ &= s(e_1,e_2)(\lambda\varepsilon - \lambda\varepsilon_r + \overline{a}\varepsilon + bu + \Delta a\varepsilon - \dot{\varepsilon}_r).\end{aligned}$$

Here we have used the fact that $\dot{e}_1 = e_2$. The design of the controller ensures that this function has a negative definite derivative so that $s \to 0$, which in turn implies asymptotic convergence of the error trajectories to 0.

The first component of the classical sliding mode controller is called the equivalent control and labeled u_{eq}. This is defined to cancel the nominal / known terms in $\dot{s}$. That is, if we set $\Delta a\varepsilon = 0$, u_{eq} is the u which results in $\dot{s} = 0$, so that

$$u_{eq} = -\frac{\lambda\varepsilon - \lambda\varepsilon_r + \overline{a}\varepsilon - \dot{\varepsilon}_r}{b}.$$

This ensures the level set of error trajectories satisfying $s(e_1, e_2) = 0$ is invariant as long as the uncertain terms in the system are compensated.

Since the uncertain terms in the system are by definition unknown, we determine a bound on these terms. In our case we have $\Delta a\varepsilon \leq \Delta a_{max}|\varepsilon|$ so we define the

$$u_{sw} = -\frac{1}{b}\big(\Delta a_{max}|\varepsilon| + \eta\big)\text{sign}(s(e_1,e_2))$$

where $\eta > 0$ is a design parameter affecting the speed of convergence of $s \to 0$ and sign() is the function which is 1 for positive arguments, -1 for negative arguments, and 0 otherwise. Setting $u = u_{eq} + u_{sw}$, the Lyapunov function satisfies

$$\begin{aligned}\frac{d}{dt}\frac{s^2}{2} &= s\dot{s} \\ &= s(\lambda\varepsilon - \lambda\varepsilon_r + \overline{a}\varepsilon + bu_{eq} + bu_{sw} + \Delta a\varepsilon - \dot{\varepsilon}_r) \\ &= s(\Delta a\varepsilon - \big(\Delta a_{max}|\varepsilon| + \eta\big)\text{sign}(s)).\end{aligned}$$

When s is positive, $\Delta a\varepsilon$ is subtracted by a term which is guaranteed to be larger than it, resulting in a negative value multiplied by the positive s and $\frac{d}{dt}s < 0$. The result is similar when s is negative so convergence to $s \to 0$ is guaranteed, as is convergence of $e_1 \to 0, e_2 \to 0$.

To test the control, the closed loop model was simulated with the reference trajectory set to a 2kHz sine wave at an offset of 2×10^{-4} and amplitude 2×10^{-5}. A normally distributed measurement noise with standard deviation $\sigma = 10^{-6}$ was added to the state observations used for computing the control value to simulate measurement noise. The control parameters were set to $\lambda = 10^7, \eta = 10^{-3}$. Figure 4 shows the results, which demonstrate good tracking performance with relative errors generally below 3%.

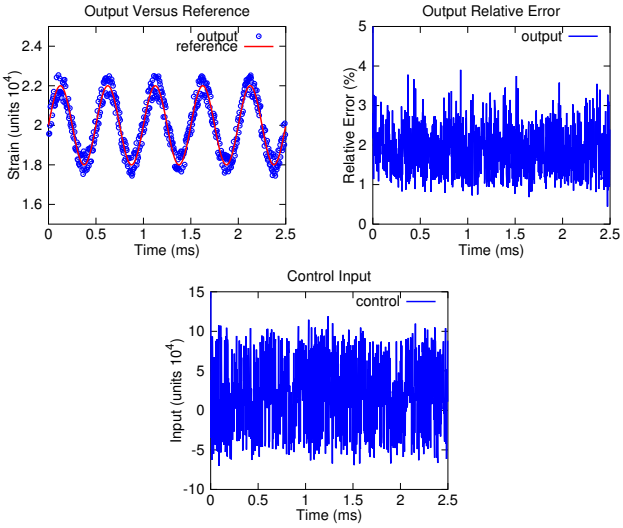

Fig. 4. (Left) Output of closed loop system compared with the reference trajectory. (Right) Relative output error. (Bottom) Input signal.

5. CONCLUSIONS

In this paper, we adapted the methodology for designing a sliding mode controller using parameteric uncertainty quantification, first presented in Crews et al. [2012], to a ferroelectric actuator system. Using synthetically generated random values to simulate measurement noise, we illustrated estimation of the parameter distribution using Bayesian inference and demonstrated the proper functioning of the sliding mode controller in the simulated closed loop system. Certain caveats for our approach apply. One is that the system model must be accurate enough that it is reasonable to assume the measurement errors are well-represented as i.i.d. Gaussian noise (adjustments for non-Gaussian noise are possible). Another is that for a practical system, a term bounding the measurement noise should also be added to the system uncertainty bound since generally uncertainty in the model parameters only partially determines the prediction intervals in which data are expected to lie. A final note is that while the controller simulation results demonstrate the feasibility of the approach, they are somewhat limited due to the large value of a used in the system (which was determined from a physical actuator). This results in a small time-constant for the system so that the effects of chattering in the controller and the simulated noise are less important. We reiterate, however, that experimental results for an analogous shape-memory alloy actuator system published in Crews et al. [2013] have verified the real-world practicality of this approach which gives reason to believe the same will hold true for ferroelectric actuator systems, as well. Experimental testing of such a system remains future work.

REFERENCES

Xinkai Chen and Takeshi Hisayama. Adaptive sliding-mode position control for piezo-actuated stage. *IEEE Transactions on Industrial Electronics*, 55(11):3927–3934, 2008.

J. H. Crews, R. C. Smith, and J. C. Hannen. Development of robust control algorithms for shape memory alloy

bending actuators. In *Proceedings of the ASME 2012 Conference on Smart Materials, Adaptive Structures, and Intelligent Systems, SMASIS 2012*, Stone Mountain, GA, 2012.

John H Crews, Jerry A McMahan, Ralph C Smith, and Jennifer C Hannen. Quantification of parameter uncertainty for robust control of shape memory alloy bending actuators. *Smart Materials and Structures*, 22(11): 115021, 2013.

Zhengzheng Hu, Ralph C Smith, Nathanial Burch, Michael Hays, and William S Oates. A modeling and uncertainty quantification framework for a flexible structure with macrofiber composite actuators operating in hysteretic regimes. *Journal of Intelligent Material Systems and Structures*, 2013. doi: 10.1177/1045389X13489781.

Hwee Choo Liaw, Bijan Shirinzadeh, and Julian Smith. Enhanced sliding mode motion tracking control of piezoelectric actuators. *Sensors and Actuators A: Physical*, 138(1):194 – 202, 2007.

Jerry A McMahan, John H Crews, and Ralph C Smith. Inversion algorithms for the homogenized energy model for hysteresis in ferroelectric and shape memory alloy compounds. *Journal of Intelligent Material Systems and Structures*, 24(15):1796–1821, 2013. doi: 10.1177/1045389X12471868.

G. Monsees and J. Scherpen. Adaptive switching gain for a discrete-time sliding mode controller. In *American Control Conference, 2000. Proceedings of the 2000*, volume 3, pages 1639 –1643 vol.3, 2000. doi: 10.1109/ACC.2000.879479.

F. Plestan, Y. Shtessel, V. Brgeault, and A. Poznyak. New methodologies for adaptive sliding mode control. *International Journal of Control*, 83(9):1907–1919, 2010. doi: 10.1080/00207179.2010.501385.

J.-J. E. Slotine and W. Li. *Applied Nonlinear Control*. Prentice Hall, Englewood Cliffs, NJ 07632, 1991.

R. Smith. *Smart Material Systems: Model Development*. SIAM, Philadelphia, PA, 2005.

Ralph C Smith. *Uncertainty Quantification: Theory, Implementation, and Applications*. SIAM, Philadelphia, PA, 2014.

Ralph C Smith and Zhengzheng Hu. Homogenized energy model for characterizing polarization and strains in hysteretic ferroelectric materials: Material properties and uniaxial model development. *Journal of Intelligent Material Systems and Structures*, 23(16):1833–1867, 2012. doi: 10.1177/1045389X12453967.

Mohammad Sheikh Sofla, Seyed Mehdi Rezaei, Mohammad Zareinejad, and Mozafar Saadat. Hysteresis-observer based robust tracking control of piezoelectric actuators. In *2010 American Control Conference*, pages 4187–4192, Baltimore, MD, USA, June 2010.

A. M. Stuart. Inverse problems: A bayesian perspective. *Acta Numerica*, 19:451–559, 5 2010. ISSN 1474-0508. doi: 10.1017/S0962492910000061.

Vadim I. Utkin. *Sliding Modes in Control Optimization*. Communications and Control Engineering Series. Springer-Verlag, Berlin Heidelberg New York, 1992.

Qingsong Xu and Yangmin Li. Global sliding mode-based tracking control of a piezo-driven xy micropositioning stage with unmodeled hysteresis. In *The 2009 IEEE/RSJ International Conference on Intelligent Robots and Systems*, pages 755–760, St Louis, USA, October 2009.

S. Yu, X.Yu, and M. Efe. Modeling-error based adaptive fuzzy sliding mode control for trajectory-tracking of nonlinear systems. In *Industrial Electronics Society, 2003. IECON '03. The 29th Annual Conference of the IEEE*, volume 3, pages 3001 – 3006 Vol.3, Nov. 2003. doi: 10.1109/IECON.2003.1280726.